PHILOSOPHICAL TRANSACTIONS A

rsta.royalsocietypublishing.org

Review

**Cite this article:** Wünnemann K, Weiss R. 2015 The meteorite impact-induced tsunami hazard. *Phil. Trans. R. Soc. A* **373**: 20140381. http://dx.doi.org/10.1098/rsta.2014.0381

Accepted: 31 July 2015

One contribution of 14 to a theme issue 'Tsunamis: bridging science, engineering and society'.

**Subject Areas:**
geophysics, oceanography, fluid mechanics

**Keywords:**
meteorite impact, tsunami, numerical modelling, Eltanin, natural catastrophe, impact hazard

**Author for correspondence:**
K. Wünnemann
e-mail: k.wuennemann@mfn-berlin.de

# The meteorite impact-induced tsunami hazard

K. Wünnemann[1] and R. Weiss[2]

[1]Museum für Naturkunde Berlin, Leibniz Institute for Evolution and Biodiversity Science, Invalidenstrasse 43, Berlin 10115, Germany
[2]Department of Geosciences, Virginia Tech, Blacksburg, VA 24061, USA

When a cosmic object strikes the Earth, it most probably falls into an ocean. Depending on the impact energy and the depth of the ocean, a large amount of water is displaced, forming a temporary crater in the water column. Large tsunami-like waves originate from the collapse of the cavity in the water and the ejecta splash. Because of the far-reaching destructive consequences of such waves, an oceanic impact has been suggested to be more severe than a similar-sized impact on land; in other words, oceanic impacts may punch over their weight. This review paper summarizes the process of impact-induced wave generation and subsequent propagation, whether the wave characteristic differs from tsunamis generated by other classical mechanisms, and what methods have been applied to quantify the consequences of an oceanic impact. Finally, the impact-induced tsunami hazard will be evaluated by means of the Eltanin impact event.

## 1. Introduction

The impact of a meteorite is the most devastating natural catastrophe due to the magnitude of the consequences that can be global and the multitude of different hazards that are created by impacts. However, strikes of large cosmic objects, which are objects with diameters larger than hundreds of metres, occur very infrequently. Only about 185 impact structures are known from the geological record (Earth Impact Database: http://www.passc.net/EarthImpactDatabase/). A more complete record of the cosmic bombardment that the Earth has suffered in the geological past can be found on the Moon, whose surface is peppered with crater structures because it has been inactive for the last 3 billion years. Three main reasons can be

THE ROYAL SOCIETY PUBLISHING

identified for the lack of craters on the Earth: (i) the geologically active nature of our planet (exogene and endogene dynamics) and the constant recycling of oceanic crust by subduction, (ii) the atmosphere, which is capable of deflecting small bodies, and (iii) the fact that about two-thirds of the Earth's surface is covered by water. For the last point, direct evidence of impacts, such as crater structures [1–5] or indicative high-pressure modifications in rocks and mineral phases [6,7] on the ocean floor, can only be found if an impactor is large enough to penetrate through the water column [7–9]. The exact diameter that a meteorite has to have to leave behind physical evidence on the seafloor is being discussed in the literature, but estimates from numerical modelling (e.g. [3,10]) and experimental work [1,5] indicate that the diameter has to be at least 10–15% of the water depth, assuming a rocky composition and an average impact velocity of 18 km $s^{-1}$ ([9] and references therein). From these rough estimates, it can be concluded that bodies smaller than approximately 500 m falling into an ocean with a typical water depth of 3.5–4 km do not leave any trace behind. As an example for a threshold case, the Eltanin impact in the Bellinghausen Sea (2.15 Ma [11,12]) is the only verified impact in deep ocean waters.

As mentioned above, another reason for the paucity of impact structures on the ocean floor is the constant recycling of oceanic crust by subduction. The older sections of the oceanic crust do not exceed more than 200 Myr, which is a short period of time to be exposed to the influx of cosmic bodies. Relative to the ocean floor, the continental shelf regions are much older, which explains the larger number of 15–20 impact structures that are thought to have formed underwater, but in the continental crust [13].

Independent of whether the impact evidence in the ocean crust is lost or whether the impact was too small to form a crater on the ocean floor, any body impacting the ocean will result in large waves that propagate away from the impact site. These large tsunami-like waves can then create tsunami sediments with which indirect identification and reconstruction of the strike of a cosmic body in a marine environment can be achieved (e.g. [9]). Therefore, the quantitative understanding of the generation, propagation and run-up of impact-generated tsunami waves is not only important to quantify the hazard and risk posed by impacts into oceans, but also is imperative for the reconstruction of the Earth's impact record.

The most likely impact scenario is a body that is just big enough to travel through the atmosphere and impact the deep-marine environment. The threshold diameter to traverse the atmosphere is about 200 m for rocky and about 50 m for iron asteroids [14,15]. Such a body would not do much damage on land [16–18], but would certainly have a much greater impact if it fell into deep water. However, the frequency (e.g. [19]) and the actual range of possible tsunami amplitudes of these small-diameter impacts is a matter for discussion (e.g. [9,20–22] and references therein).

In this contribution, we summarize the different approaches that are employed to study the generation, propagation and run-up of impact-induced tsunami waves.

## 2. Mechanisms of wave generation

The strike of a cosmic body is governed by a slew of complex processes (e.g. [23,24]) that can simply be ascribed to the hypervelocity of the impact itself (about 18 km $s^{-1}$). The main result of the hypervelocity impact is the formation of a crater that is a consequence of the generation of shockwaves. Shockwaves are waves whose speed is greater than the speed of sound for the material through which they travel. This paper focuses on the tsunami waves generated during an impact in the marine environment; however, a basic comprehension of shockwaves and crater mechanics is essential for a better understanding of the different generation mechanisms of tsunami-like waves. Figure 1 depicts the generation of tsunami waves after the vertical impact of a body into deep (left) and shallow (right) water.

To describe the processes that result in the formation of craters and tsunami waves, meteorite impacts are often compared to the detonation of explosives. It might not be intuitively clear why an explosion is an appropriate analogue for studying hypervelocity impacts. The fact, however,

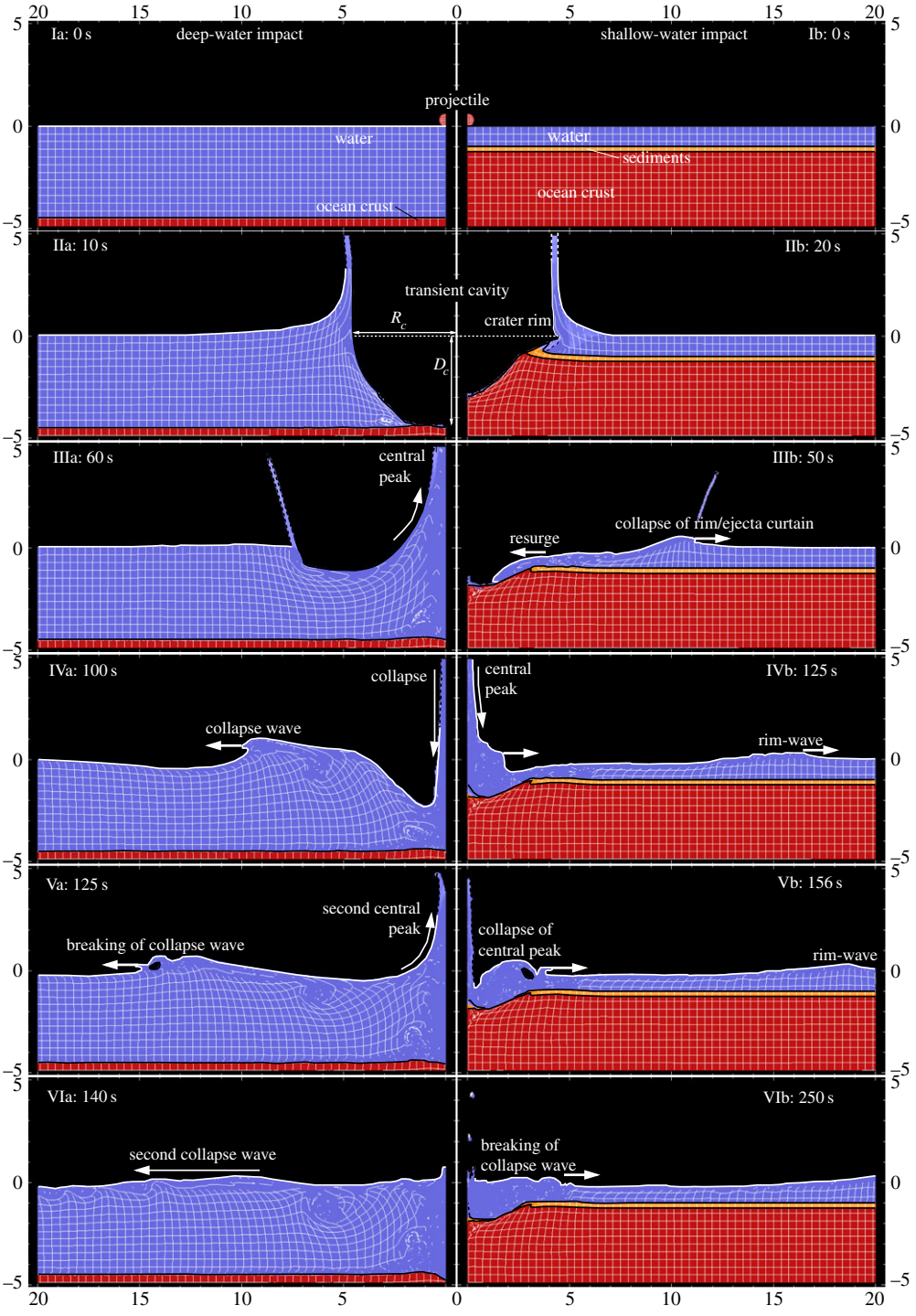


**Figure 1.** Snapshot series of (left, a) a deep-water and (right, b) a shallow-water impact with $L/h = 0.22$ and $L/h = 0.6$. Blue (grey) indicates the water column, orange (light grey) indicates a thin layer (250 m) of water-saturated sediments (right-hand column only) and red (dark grey) indicates the basement. The overlaid grid depicts the deformation. In regions where mixing and turbulent flows occur, no grid is plotted. $R_c$ and $D_c$ mark approximately the radius and depth of the transient crater, respectively. Models are taken from Wünnemann *et al.* [25] and were reprocessed and re-plotted. (Online version in colour.)

that the source of shockwaves in both cases can be approximated by a point source is the leading argument. This argument allows the results of underwater explosion experiments carried out by Van Dorn *et al.* [26] to be used, and Glasstone & Dolan [27] employed this argument to carry out the first experiments to quantify the generation and propagation of waves in marine impacts. How the shockwaves interact with the material through which they travel is complex: the impact velocity $U$ is larger than the speed of sound $c_B$. The shockwaves are first generated during the penetration of the projectile into the water column, compressing both the water and the projectile. A large fraction of the initial kinetic energy of the projectile is transferred to the water by shock compression (internal energy). After the release from high shock pressure, the remaining internal energy causes vaporization of water, and a fraction of the energy is transferred back into kinetic energy triggering a radial flow of water. This flow field is similar to that generated by an explosion at some depth beneath the water surface. The result of the flow field is the excavation of a crater of paraboloid shape. Some of the excavation-flow trajectories end above the pre-impact surface, indicating ejecting water. The spray of ejected water, the so-called ejecta curtain, changes state towards its interior into an expanding plume of water vapour. At its toe, there is a continuous transition to an elevated crater rim. The shock-induced excavation of the crater is more efficient than the displacement of water due to the penetration of the meteorite downward, which is why in a hypervelocity impact the resulting crater is much larger than in a low-velocity impact where no shockwaves are involved and the extent of the crater is of the same size range as the projectile itself. Obviously, the radial flow is slowed down and stopped by buoyant forces due to gravity. At the point when radial flow stops, the crater will have its largest extent, which is defined as the transient crater, $R_c$. The transient crater usually is 20–40 times larger than the diameter, $L$, of the projectile. Because of the energy of the flow that generates the transient crater, its radius $R_c$ is directly proportional to the kinetic energy of the impact. After the radial flow has stopped, the buoyant forces then cause a second radial flow directed towards the impact centre. This centripetal flow field converges at the centre of the transient crater, forming an upward rising central peak of water (figure 1).

Primarily, two different mechanisms are responsible for the generation of waves during impact crater formation in an oceanic target ([1,25], figure 1), as follows.

(1) The ejecta curtain (spray; figure 1 IIa and IIb) eventually collapses (figure 1 IIIa and IIIb), and a dense layer of water particles that were initially thrown out of the crater at velocities of hundreds of metres per second re-impact on the surface at a velocity similar to the ejection velocity. The plunging of the ejecta curtain on the water surface generates the first wave signal that propagates away from the crater, the so-called rim wave (figure 1 IIIb–Vb). The amount of water displaced by this process may be comparable to the amount of water in a circular trough that reaches down to about one-third of the transient crater depth, the so-called excavation depth. As a rough estimate, the total ejected mass corresponds to one-quarter of the total mass displaced from the transient crater.
(2) The collapse of the transient crater by centripetal infill of the crater from the adjacent ocean (figure 1 IIa) results in the formation of a central peak or jet of water reaching far above the pre-impact surface (figure 1 IIIa). This vertical jet at the centre of the transient crater is generated by the same mechanism that causes a splash after a stone falls into water. The gravitational collapse of the central jet generates another wave, the so-called collapse wave (figure 1 IVa). In fact, the formation of the central jet and subsequent collapse may repeat several times (figure 1 IVa–VIa), and a train of collapse waves is formed [25]. Note that the first signal originating from the collapse is a wave trough (figure 1 IVa), because of the inward directed flow field, and it may cancel out the first signal of the rim wave. The amount of water displaced by this process may be comparable to the total mass displaced from the transient crater (see [28,29] for simple analytic estimates of the size of the transient crater relative to the kinetic energy of the impactor).

The formation of the rim and collapse waves strongly depends on the ratio between the water depth and the size of the transient crater. In so-called shallow-water impacts (figure 1 Ib–VIb), where the diameter of the impactor is comparable to the depth of the water, the effect on crater formation by the water column is negligible. In this case, the mass of ejected material consisting of some water but primarily of lithic fragments from the ocean floor dominates over the mass of water displaced by the formation of a crater, and the rim wave is much more pronounced than the collapse wave. Prominent examples of such a scenario that have been investigated in terms of the generated waves and associated potential deposits at the coast are the Chicxulub impact [30,31], the Chesapeake Bay impact [9,32,33], the Lockne impact [34,35] and the Mjolnir impact [10,36]. In so-called deep-water impacts, where the transient crater does not reach the ocean floor, the collapse wave dominates over the rim wave. This is because the mass of the transient crater is approximately three times the mass of the ejecta curtain, and the wave trough of the collapse wave overlaps with the wave crest of the rim wave. Although this is the most likely scenario (70% of the Earth's surface is covered with deep oceans and relatively small objects are much more frequent than large impactors), the only known example is the aforementioned Eltanin impact.

The transition from shallow-water to deep-water impacts is gradual. It is linked to the kinetic energy of the impactor and, therefore, depends on the composition of the projectile (iron meteorites penetrate deeper into the water than similar-sized stony meteorites at the same velocity). Furthermore, the impact angle is important. Generally, the higher the impact velocity $U$ and steeper the angle $\alpha$, the deeper the projectile penetrates into the water column (an impact velocity of $U = 18\,\mathrm{km\,s^{-1}}$ and $\alpha = 45^{\circ}$ are the most likely parameters). The intermediate regime between shallow-water and deep-water impacts may range from $L/h = 1$ to $L/h = 0.17$, where $L$ is the projectile diameter and $h$ is the water depth [9].

In fact, the vast majority of impacts occur at an oblique impact angle. However, the most often studied case (experimentally and through numerical models) is the very unlikely vertical strike of a bolide (figure 1). In a vertical impact, the perfect cylindrical symmetry, where the collapse of the transient cavity occurs in all radial directions at the same time, causes an implausibly high central jet of water (figure 1IIIa and IVb), that later collapses to drive an outward going wave. No impact is truly vertical, and even in a slightly oblique impact the inrushing water does not meet exactly at the centre, spoiling the high symmetry needed to produce the kind of jet illustrated in figure 1. Full three-dimensional simulations do not show this effect (e.g. [2,37,38]) as the collapse in the downrange direction starts a little later than in the uprange direction, which causes deviations from perfect symmetry. An example of a simulation of an oblique impact is shown in figure 2. However, such models are computationally expensive and systematic studies on the effect of the impact angle on the height of the central splash are lacking, yet.

Aside from the impact angle, the local topography at the impact site might also be important for the formation of tsunami-like waves. In a recent modelling study, Shuvalov & Gersonde [39] demonstrated that neither topography nor impact angle affects the wave characteristic significantly in the far field. At some distance from the point of impact, the wave generated by an oblique impact becomes more or less circular-symmetric [10]. Close to the point of impact, the height of the generated waves is a function of the impact angle and water depth.

Finally, it should be mentioned that atmospheric effects may also be important. The atmosphere, heated and turbulent both from the pre-impact passage of the bolide and from the sudden injection of enormous quantities of vaporized water, can, on the one hand, be an additional mechanism to generate waves and, on the other hand, may dampen the waves originating from the ejecta curtain plunging onto the water surface [40]. A useful analogy can be made with the Krakatoa eruption, in which the atmospheric pressure wave generated waves that could be traced in all the ocean basins of the world [40]. Depending on the location of an impact, the wave effects on nearby shores could be much more similar to storm surges than to classical tsunamis [40].

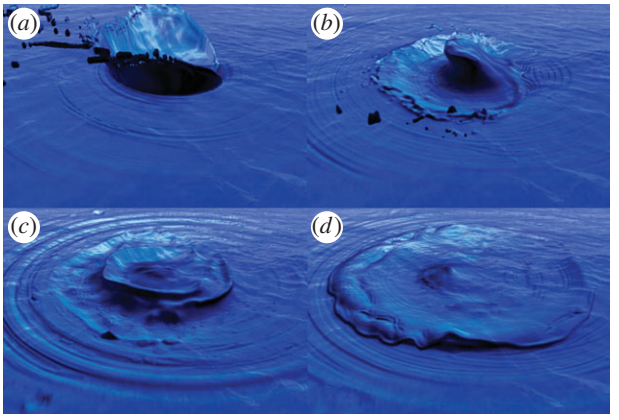


**Figure 2.** Snapshot series of a three-dimensional simulation of an oblique impact (45°) into deep water ($L/h = 0.04$) at 12 km s$^{-1}$. The asymmetric collapse of the transient crater results in a much smaller central jet (*b*) than the axisymmetric two-dimensional simulation shown in figure 1IVb (D. Elbeshausen 2012, personal communication). (Online version in colour.)

# 3. Wave characteristics and propagation

## (a) Wave characteristics of impact-generated tsunami waves

As mentioned earlier, the generation mechanisms of tsunami waves determine their characteristics and therefore their fate as they travel far distances across the oceans. The tsunami-generating processes not only govern the characteristics of the individual tsunami waves, but also determine the properties of the tsunami wave train that is created, especially the number of significant waves. For example, the water surface deformation due to earthquakes can engulf large areas, but the vertical displacement generally does not exceed a few metres; however, in extreme cases, 10 m is possible. It is important to note that the length of time during which the seafloor is deformed is such a tiny fraction of the time scale of the subsequent tsunami that its dynamics does not need to be considered in the analysis of the wave generation process. The number of significant earthquake-generated tsunami waves by a single event is rarely larger than two or three.

The generation of tsunamis during submarine landslide is very different. In this case, the time scale of the wave-forming processes has magnitudes that make it necessary to consider the forcing mechanism. Then, together with the velocity of the slide motion, the waves that are generated have a smaller period and are larger in amplitude. Because of their amplitude and period, these waves have nonlinear properties, which means that wave energy is constantly shifting from longer to shorter periods as the waves propagate away from the generation area. This effect is referred to as dispersion, which we will consider later.

The wave generation mechanisms, described in the previous section, result in the formation of waves (rim and collapse waves) that initially can be hundreds of metres in amplitude with comparatively short periods. Of course, these waves are also nonlinear and the same shift of wave energy occurs as in the case of landslide-generated tsunami waves. However, very close to the impact area, the wave height can have the same order as the water depth. Waves of such amplitude cannot propagate, but are reduced by breaking into amplitudes at which propagation is possible. Impact-generated tsunami waves do not have characteristics that can be scaled up from landslide-generated waves. Their amplitude is disproportionately larger. Therefore, impact-generated tsunami waves behave much more nonlinearly. Their attenuation is different from landslide-generated waves, and they are very demanding in terms of computational resources and wave theory to explore their dynamics as they propagate away from the impact site.

Considering the spectrum of tsunami waves near the generation area, earthquake-generated tsunamis have the longest periods and the smallest amplitudes, and impact-generated tsunamis

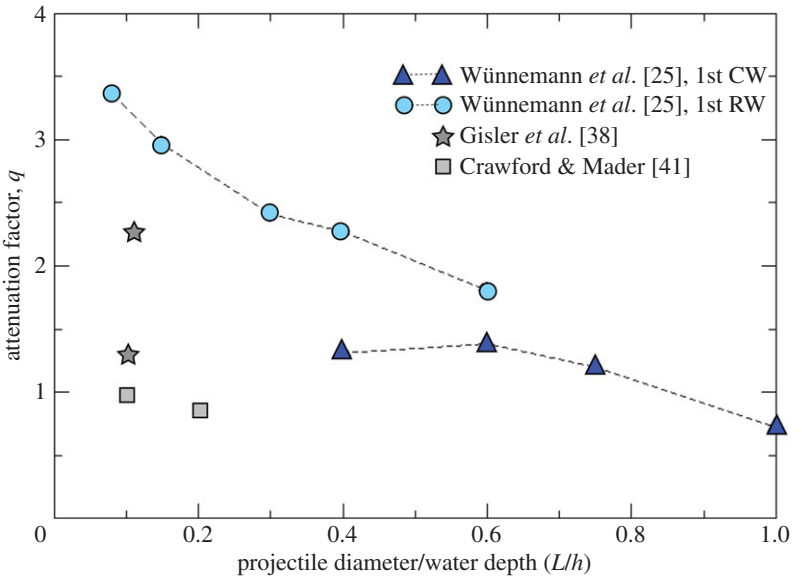


**Figure 3.** Attenuation factor $q$ as a function of impactor diameter–water depth ratio $L/h$ (after [25]). The attenuation factor was determined for the maximum wave height of the rim wave (RW) and the collapse wave (CW) separately in models of impacts into different depths of water (cf. figure 1). In an intermediate region, $0.4 < L/h < 0.6$, both wave types, rim and collapse, exist. For comparison, the attenuation factor $q$ from other modelling studies [38,41] is included. (Online version in colour.)

have relatively short periods and very large amplitudes. Therefore, we can conclude that earthquake-generated waves are the most linear and impact-generated waves are the most nonlinear tsunami waves. This has consequences for the propagation and the evolution of the wave characteristics as both tsunami types travel across an ocean.

## (b) Propagation of impact-generated tsunami waves

The propagation of waves depends on the wave characteristics and their interaction with the local bathymetry. The evolution of earthquake-generated tsunami waves is usually considered for each wave separately because their number is so small. These waves are linear and their attenuation is proportional to $r^{-0.5}$, where $r$ represents an increasing distance to the generation area. The square root indicates that the increasingly larger area, the wave field engulfs, is responsible for the amplitude decay. This effect is known as geometric spreading. For nonlinear waves, for example those generated during landslides or by meteorite impacts, the attenuation is generally proportional to $r^{-q}$, where $q$ has values larger than 0.5. For landslide-generated tsunami waves, the value of $q$ is approximately 1. However, for impact-generated tsunami waves, the value $q$ can vary greatly and may change with distance. Wünnemann *et al.* [25] presented a study which showed that $q$ depends on the ratio between the diameter of the impactor and the local water depth when impact energy is kept constant. According to this modelling study, $q$ varies between 0.8 and 3.4 (figure 3).

The reason for these different $q$ values can be found in the waves themselves, especially in the profile of the horizontal component of the wave orbital velocity. Small $q$ values are associated with orbital velocities that do not show any change with depth, which is characteristic for classic shallow-water waves. However, for larger values of $q$, especially for $q > 1$, the profile of the horizontal velocity resembles that which can be found for deep or intermediate deep-water waves. Figure 4 depicts two different examples for $q = 3$ and $q = 1.2$.

The impact-generated tsunami waves that have a horizontal velocity profile similar to profiles found in deep or intermediate deep-water waves are associated with deep-water impacts, where the collapse of the water cavity dominates the generation process of tsunami waves (collapse

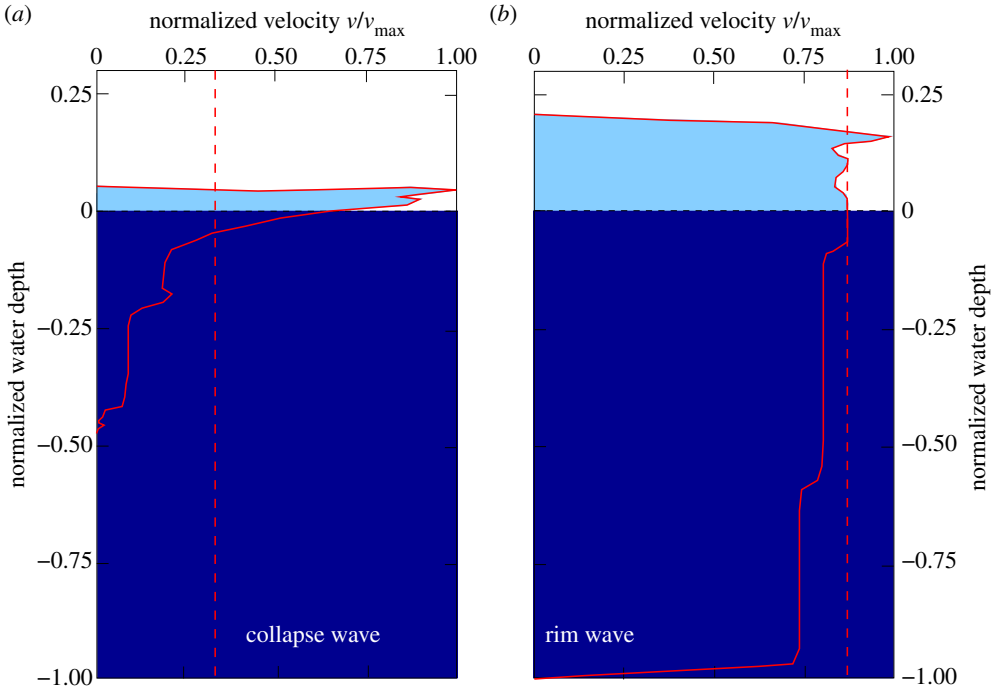


**Figure 4.** Vertical profile through the water column of the radial velocity component (*a*) for the collapse wave ($r = 19.6$ km and $t = 300$ s) at a deep-water impact ($L/h = 0.15$) with an attenuation factor $q = 3$ (figure 3) and (*b*) for the rim wave ($r = 38$ km, $t = 300$ s) at a shallow-water impact ($L/h = 0.75$) with an attenuation factor $q = 1.2$. The dashed lines mark the theoretically determined velocity of a shallow-water wave: $v = A(g/h)^{0.5}$, where $A$ is the wave amplitude, $g$ is gravity and $h$ is water depth. Adapted from Wünnemann *et al.* [25]. (Online version in colour.)

waves). Those impact-generated waves that have horizontal velocity profiles similar to those of classic shallow-water waves are associated with shallow-water impacts, and the collapse of the rim plunging onto the water surface dominates the generation process of the so-called rim waves. It should be noted that while, for the latter waves, the vertical profile of the horizontal velocity is similar to the profile of earthquake-generated waves, they are not linear waves because their relatively short wave period causes nonlinear processes to be present and grow during the propagation process. During the propagation of these waves, energy is shifted from the long waves to shorter components of the wave frequency spectrum (dispersion), and a tail of waves is generated that is referred to as the dispersive tail.

To simulate the propagation of impact-generated tsunami waves, the governing equations of the respective wave theories must be able to handle nonlinear waves and the different profiles of the horizontal velocity. The Boussinesq wave theory is an excellent candidate for such a theory. However, the nonlinear processes that result in dispersion acting on time and length scales require very fine temporal and spatial resolutions on top of the demanding wave theory required to adequately simulate the wave dynamics. The next section will cover some of the prominent approaches to study the evolution of impact-generated tsunami waves.

## 4. Quantitative assessment

Numerous attempts have been made to quantify impact-generated tsunami waves, including the formation of waves, how they propagate across the ocean and the run-up process at the coast. The fact that no conclusive answer has been found to the question of whether impacts in the

marine environment produce mega-tsunamis of greater dimensions than any other generation mechanism is due to deviating results from different methodological approaches.

## (a) Analogue experiments

The first estimates are based on underwater nuclear explosion experiments suggesting an empirical relationship between the energy $Y$ equivalent of kilotonnes of TNT (1 kt TNT $= 4.186 \times 10^{12}$ J; in an impact event, the energy corresponds to the kinetic energy of the impactor), the wave amplitude $A$ as a function of distance $r$, and water depth $h$ [27]: $A = 45(h/r)(Y)^{0.25}$. Gault & Sonett [1] found similar scaling laws by conducting impact experiments with water-covered targets in the laboratory.

Based on larger scale explosion experiments to study waves, Van Dorn *et al*. [26] recognized that nonlinear wave shoaling of large amplitude is an effective process to dissipate wave energy. The so-called 'Van Dorn effect' implies that explosion-generated, and, thus also impact-generated, tsunami waves attenuate quickly due to wave breaking and other nonlinear processes as the wave travels across a scaled continental shelf. The Van Dorn effect has not been considered in estimates of the impact-induced tsunami hazard, leading to overprediction of run-up heights until Melosh [20] raised the point (see also further discussion in §4c).

## (b) Analytical approach: wave theory

Linear wave theory can be employed to analytically approach the propagation of impact-induced tsunamis. Ward and Asphaug [21,22,42] assumed in their analytical study of impact-induced wave propagation that only linear processes act on the waves as they propagate away from the impact site. For the analytical solution, scaling laws are employed to estimate the transient crater size. These scaling laws work best for impacts in deep water assuming a parabolic crater shape. Other scaling laws exist to estimate the initial height of the ejecta curtain [28]. However, asymmetric effects due to an oblique angle of impact or bathymetry are neglected. If the transient crater in the water column reaches the ocean floor and a crater is formed in the strata and the crust underneath, scaling laws no longer can be used to estimate initial conditions (crater size and ejecta curtain height) for linear analytical approaches. Ward & Asphaug [21] used an approximated shape function of the transient crater as the initial waveform and calculated by linear wave theory how this signal evolves into a tsunami-like wave propagating across the ocean. This elegant way of solving the problem analytically allows for predicting the wave attenuation as a function of distance in a relatively straightforward way. However, the exclusion of any nonlinear process might be considered an oversimplification, especially in areas where the waves interact with bathymetric features and when the waves propagate into shallow-water depth. Another problem in the analytic approach is the assumption that the initial waveform can be approximated by estimates of the maximum extent of the transient crater in terms of depth, diameter and rim height. Although well-established scaling laws provide good estimates of these parameters, it has to be considered that the transient crater does not exist at a certain point in time (snapshot of the crater formation process), but has to be understood as a virtual construct helping to relate the impact energy to some measure of the crater formation process. In other words, the morphometric parameters of the transient crater cannot be determined at a certain point in time. The difference between the extent of the transient crater and the actual size and shape of the growing cavity in the water column becomes more pronounced with decreasing crater efficiency (the ratio of the crater mass and the mass of the projectile; the ratio decreases with the size of an impact event) and the angle of impact. For instance, the crater radius $R$ at a given point in time is still growing ($R < R_c$, figure 1), while the maximum depth ($D_c$, figure 1) has already been reached and the floor rises upwards due to gravity collapse (see also the description in §2). The hiatus between collapse of the crater floor, inflow from the adjacent ocean, and collapse of the ejecta curtain affects wave generation significantly. The simplified initial conditions used in the analytical approach by

Ward & Asphaug [21] may, therefore, be the reason for extremely large and probably implausible initial wave amplitudes—larger than those found in most other studies using other approaches.

## (c) Numerical modelling

The specific characteristics of impact-induced waves make it rather difficult to use numerical tools that are very suitable for earthquake- and even in some regards landslide-generated tsunami waves. The wave generation process and the very early wave dynamics is highly nonlinear and complex. Not even very high order wave theories are capable of reliably describing the early wave evolution. Therefore, the wave generation and early wave evolution must be part of the model framework that considers hypervelocity impacts and cratering processes. Only a relatively small number of codes exist that are capable of dealing with hypervelocity impact processes and only a very few of them have been used to study meteorite impact processes. For a summary of so-called hydrocode modelling, see, for example, [43] and references therein. Although hydocodes are able to simulate generation, propagation and inundation of impact-induced tsunami waves, this approach would be computationally too expensive to cover the whole sequence of processes. In fact, only a few examples of hydrocode modelling are published where the propagation of waves was tracked as far as 100 times the diameter of the projectile (e.g. [37–40]). For the most likely scenario of a relatively small object of a few hundred metres in diameter wave propagation can be simulated only to a distance of tens of kilometres with such an all-in-one model approach.

The multi-scale nature of impact-induced tsunami waves suggests the usage of different models appropriate to deal with the specific processes on different spatio-temporal scales, such as generation, propagation including shoaling and run-up, separately. Crawford & Mader [41] were the first to employ such a hybrid approach by combining CTH hydrocode modelling of crater formation with the ZUNI code for wave propagation simulation. Following this approach, Weiss *et al.* [44] coupled iSALE hydrocode modelling with a Boussinesq-type wave propagation code and the MOST model, allowing quantitative predictions of inundation and run-up heights. Both studies suffer from the fact that wave propagation did not take a realistic bathymetry into account.

A critical and difficult part is always the coupling between different models and thorough testing is crucial to make sure that no numerical artefacts result from the change from a high-resolution computational domain (either full three or two dimensions with cylindrical geometry) where the compressible Navier–Stokes equations are solved (region of crater formation) to the computational domain where material flow is calculated by shallow-water or Boussinesq approximation on a two-dimensional grid (longitude and latitude). In commonly used tsunami propagation models, the wave height and water depth are functions of longitude and latitude, and the actual thickness of the water column and flow velocities as a function of depth are not resolved. Such models are only applicable to waves longer than 10–20 times the water depth. Shorter waves (typical for impacts) with a wavelength-to-depth ratio of 2 or greater can be modelled with pCOULWAVE [45]. The code considers the varying orbital velocity $v$ as a function of depth (figure 4), allowing for a quantitative assessment of the above-mentioned Van Dorn effect. Korycansky & Lynett [46,47] used the code to investigate the behaviour of large waves approaching the continental shelf. The wave characteristic was supposed to be similar to typical collapse waves originating from a deep-water impact and was estimated according to Ward & Asphaug [21] (see also §4b). The results confirmed that waves experience shoaling and, as a consequence, they break and wave height immediately diminishes.

The successful application of the pCOULWAVE model to simulate propagation of waves with typical characteristics of impact-induced waves inspired a recently published study coupling iSALE hydrocode simulations with pCOULWAVE modelling [48]. The results of this recent state-of-the-art numerical modelling approach are shown in the next section in comparison with a selection of other results using different methodological approaches.

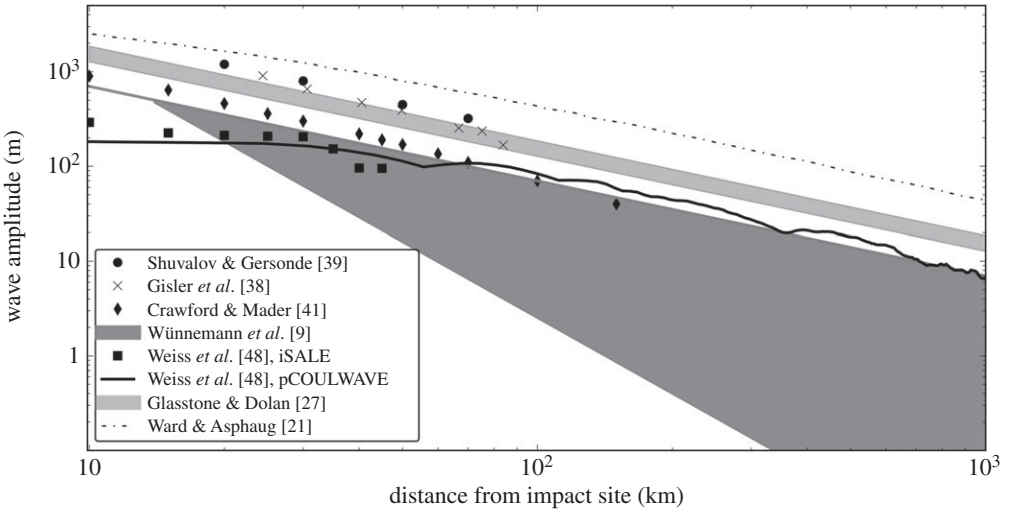


**Figure 5.** Comparison between different studies of maximum wave height as a function of distance for the Eltanin impact scenario. Shuvalov & Gersonde [39]: $L = 1000$ m, $U = 20$ km s$^{-1}$, $\rho = 3300$ kg m$^{-3}$; Weiss *et al.* [48]: $L = 750$ m, $U = 12$ km s$^{-1}$, $\rho = 2700$ kg m$^{-3}$; small-scale experiments were scaled to the impact parameters from Weiss *et al.* [48] using a transient crater radius $R_c = 5000$ km; Crawford & Mader [41]: $L = 1000$ m, $U = 20$ km s$^{-1}$, $\rho = 3300$ kg m$^{-3}$; Ward & Asphaug [21]: $L = 1000$ m, $U = 20$ km s$^{-1}$, $\rho = 3000$ kg m$^{-3}$. The grey shaded areas indicate estimates from scaling laws using impact parameters as indicated in the lower left corner.

## (d) Eltanin: a comparative example

The only known impact event in the deep ocean is the Eltanin impact that happened 2.15 Ma in the Bellinghausen Sea, Antarctica. It was only discovered by the finding of small fragments from the asteroid in drill cores [11]. Subsequent exploration of the ocean floor by parasounding revealed reworking of the seabed substrate and chaotic layering of sediments indicating strong currents associated with the collapse of the transient crater in the water column [12]. The Eltanin impact event serves as an ideal case study to investigate the most likely scenario for future impacts and the most frequent scenario of past oceanic impact events, because a relatively small object (approx. 750–1500 m in diameter) penetrated into the deep ocean, but did not reach the ground to form a crater. Because of its young age, it cannot be ruled out that deposits along the South American coast resulting from the generated waves are preserved and could be identified. However, no unambiguous tsunami deposits have been discovered and confirmed on land from the Eltanin event, or from any other oceanic impact so far. The Eltanin event was the subject of several studies gathering numerous observations [12,49,50], which were used as constraints for numerical modelling to reconstruct the event [6,7]. The two most recent studies focus on providing better constraints on the released energy [39] and on the propagation and related sediment transport competence in coastal regions of the generated waves [48]. The latter allows for an assessment of proposed tsunami deposits related to the Eltanin impact and suggests locations where high-amplitude waves hit the coast. To make such quantitative predictions hydrocode simulations of the wave generation process were coupled with the pCOULWAVE propagation model considering the present bathymetry in the South Pacific Ocean. Figure 5 shows the maximum wave height as a function of distance averaged along concentric circles around the point of impact. The wave attenuates quickly with an attenuation factor $q = 1.2$, resulting in maximum wave heights along the coast similar to the 2004 Sumatra and 2011 Tohoku tsunamis. For comparison of the results, we have included data from other studies rescaled to the Eltanin event in the figure. There appears to be an overall agreement that waves attenuate in the far field proportional to $r^{-1}$ to $r^{-1.2}$, which is also in accordance with empirical estimates from Glasstone & Dolan [27]. The main difference in the predicted wave amplitudes results from

deviations between the assumptions on the initial wave heights. While Weiss *et al.* [48] predict wave heights of the order of a couple of hundred metres in the near field, Shuvalov & Gresonde [39] determined wave heights of up to 1000 m close to the point of impact. These large differences most likely result from the fact that waves close to the point of impact are highly nonlinear, break and form bores, which makes it difficult to quantify the process. Such turbulent behaviour cannot be resolved sufficiently by existing hydrocode simulations and more appropriate modelling tools are required to quantify wave behaviour near to intermediate distance (10–100 km) from the point of impact.

## 5. Conclusion

Meteorite impacts pose a natural threat to society. If such an event occurs in a marine environment, the generation of tsunami waves would enhance the consequences by enlarging the affected area in comparison with similar size impacts on land. The question of whether the magnitude of impact-generated tsunami waves exceeds the devastation due to any other natural catastrophy such that traces of palaeo-events could be recognized in the geological record remains unanswered. On the one hand, no unequivocal evidence for impact-tsunami deposits have been found so far. Although the frequencies, in particular, of relatively small bodies impacting the Earth is a matter of debate, there is no doubt that a future impact would most likely happen in water, in which case large waves would be generated. Here, we have summarized the current state of research to quantify the magnitude of impact-generated tsunami waves in order to predict the consequences of future impacts and to aid in the detection of potential tsunami deposits of palaeo-marine impact events. Progress has been made in the characterization of the generated wave signal that resembles neither classic earthquake-generated tsunamis nor waves formed by aerial or subaerial landslides, making the application of well-established modelling tools for quantitative predictions of the propagation of waves impossible. Due to the complexity and the specifics of impact-generated waves modelling of the entire process is computationally very expensive and can only be addressed by subdividing the entire process into stages of different spatio-temporal scale. Some consensus exists concerning the attenuation of waves in the far field; however, the large variations in the wave amplitudes proposed by different authors using different methodological approaches are mainly due to differences in the initial wave amplitudes. The initial part, the generation of waves reaching as high as the depth of the ocean, is by far the most complex part and is dominated by highly nonlinear processes such as wave breaking and the formation of undular bores. Further experimental or numerical research is necessary to improve the quantitative understanding of the generation and propagation of highly nonlinear waves in the near field formed by meteorite impact.

Competing interests. We declare we have no competing interests.

Funding. We received no funding for this study.

Acknowledgements. The work described here benefited from long-term collaborations on this subject with Gareth Collins and Patrick Lynett. We are also grateful to Jay Melosh and an anonymous reviewer whose comments improved this paper. We also thank the editors for the special issue for inviting us to write this contribution.

## References

1. Gault DE, Sonett CP. 1982 Laboratory simulation of pelagic asteroid impact: atmospheric injection, benthic topography, and the surface wave radiation field. In *Geological implications of impacts of large asteroid and comets on the Earth* (eds LT Silver, PH Schultz), pp. 69–92. GSA Special Paper No. 190. Boulder, CO: Geological Society of America.
2. Shuvalov VV, Trubetskaya IA. 2002 Numerical modeling of marine impacts. *Solar Syst. Res.* **36**, 417–430. (doi:10.1023/A:1020467522340)
3. Davison D, Collins GS. 2007 The effect of the oceans on the terrestrial crater size-frequency distribution: insight from numerical modeling. *Meteorit. Planet. Sci.* **42**, 1915–1927. (doi:10.1111/j.1945-5100.2007.tb00550.x)

4. Milner DJ, Baldwin EC, Burchell MJ. 2007 Influence of a water layer on the impact cratering process and the fate of the projectile. In *Proc. of Bridging the Gap II: Effect of Target Properties on the Impact Cratering Process, Saint-Hubert, Canada, 22–26 September 2007*. LPI Contribution no. 1360, pp. 77–78. Houston, TX: Lunar and Planetary Institute.
5. Baldwin EC, Milner DJ, Burchell MJ, Crawford IA. 2007 Laboratory impacts into dry and wet sandstone with and without an overlying water layer: implications for scaling laws and projectile survivability. *Meteorit. Planet. Sci.* **42**, 1905–1914. (doi:10.1111/j.1945-5100.2007.tb00549.x)
6. Artemieva NA, Shuvalov VV. 2002 Shock metamorphism on the ocean floor (numerical simulations). *Deep-Sea Res. II* **49**, 959–968. (doi:10.1016/S0967-0645(01)00136-9)
7. Wünnemann K, Lange MA. 2002 Numerical modeling of impact-induced modifications of the deep-sea floor. *Deep Sea Res. II Top. Stud. Oceanogr.* **49**, 969–981. (doi:10.1016/S0967-0645(01)00148-5)
8. O'Keefe JD, Ahrens TJ. 1982 The interaction of the Cretaceous/Tertiary extinction bolide with the atmosphere, ocean and solid Earth. In *Geological implications of impacts of large asteroid and comets on the Earth* (eds LT Silver, PH Schultz), pp. 103–109. GSA Special Paper No. 190. Boulder, CO: Geological Society of America.
9. Wünnemann K, Collins GS, Weiss R. 2010 The impact of a cosmic body in Earth's ocean and the generation of large tsunami waves: insight from numerical modeling. *Rev. Geophys.* **48**, RG4006. (doi:10.1029/2009RG000308)
10. Shuvalov VV. 2002 Numerical modeling of impacts into shallow sea. In *Impacts in Precambrian shields* (eds J Plado, LJ Pesonen), pp. 323–336. New York, NY: Springer.
11. Kyte FT *et al.* 1981 High noble-metal concentrations in a Late Pliocene sediment. *Nature* **292**, 417–420. (doi:10.1038/292417a0)
12. Gersonde R *et al.* 1997 Geological record and reconstruction of the late Pliocene impact of the Eltanin asteroid in the Southern Ocean. *Nature* **390**, 357–363. (doi:10.1038/37044)
13. Ormö J, Lindström M. 2000 When a cosmic impact strikes the sea bed. *Geol. Mag.* **137**, 67–80. (doi:10.1017/S0016756800003538)
14. Bland PA, Artemieva NA. 2003 Efficient disruption of small asteroids by Earth's atmosphere. *Nature* **424**, 288–291. (doi:10.1038/nature01757)
15. Chyba CF *et al.* 1993 The 1908 Tunguska explosion: atmospheric disruption of a stony asteroid. *Nature* **361**, 40–44. (doi:10.1038/361040a0)
16. Toon OB, Zahnle K, Morrison D, Turco RP, Covey C. 1997 Environmental perturbations caused by the impacts of asteroids and comets. *Rev. Geophys*. **35**, 41–78.
17. Hills JG, Nemchinov IV, Popov SP, Teterev AV. 1994 Tsunami generation by small asteroid impacts. In *Hazards from comets and asteroids* (ed. T Gehrels), pp. 779–789. Tucson, AZ: University of Arizona Press.
18. Pierazzo E, Artemieva A. 2012 Local and global environmental effects of impacts on Earth. *Elements* **8**, 55–66. (doi:10.2113/gselements.8.1.55)
19. Bland PA, Artemieva NA. 2006 The rate of small impacts on Earth. *Meteorit. Planet. Sci.* **41**, 607–631. (doi:10.1111/j.1945-5100.2006.tb00485.x)
20. Melosh HJ. 2003 Impact-generated tsunamis: an overrated hazard (abstract no. 2013). In *Proc. 34th Lunar and Planetary Science Conf., Houston, TX, 17–21 March 2003*. Houston, TX: Lunar and Planetary Institute.
21. Ward SN, Asphaug E. 2000 Asteroid impact tsunami: a probabilistic hazard assessment. *Icarus* **145**, 64–78. (doi:10.1006/icar.1999.6336)
22. Ward SN, Asphaug E. 2003 Asteroid impact tsunami of 2880 March 16. *Geophys. J. Int.* **153**, F6–F10. (doi:10.1046/j.1365-246X.2003.01944.x)
23. Melosh HJ. 1989 *Impact cratering: a geological process*. Oxford, UK: Oxford University Press.
24. Collins GS, Melosh HJ, Osinski GR. 2012 The impact-cratering process. *Elements* **8**, 25–30. (doi:10.2113/gselements.8.1.25)
25. Wünnemann K, Weiss R, Hofmann K. 2007 Wave characteristics of impact-induced large waves—reevaluation of the tsunami hazard. *Meteorit. Planet. Sci.* **72**, 1–11.
26. Van Dorn WG, LeMêhauté B, Hwang LS. 1968 *Handbook of explosion generated water waves*. Report TC-130. Pasadena, CA: Tetra Tech Inc.
27. Glasstone S, Dolan PJ. 1977 *The effects of nuclear weapons*. Washington, DC: US Government Printing Office.

28. Holsapple KA. 1993 The scaling of impact processes in planetary sciences. *Annu. Rev. Earth Planet. Sci.* **21**, 333–373. (doi:10.1146/annurev.ea.21.050193.002001)
29. Holsapple KA, Housen KR. 2007 A crater and its ejecta: an interpretation of deep impact. *Icarus* **187**, 345–356. (doi:10.1016/j.icarus.2006.08.029)
30. Bahlburg H, Weiss R, Wünnemann K. 2010 Low energy sedimentary infill of the Chicxulub crater during the impact to post-impact transition. *Earth Planet. Sci.* **295**, 170–176. (doi:10.1016/j.epsl.2010.03.037)
31. Goto K, Tada R, Tajika E, Bralower TJ, Hasegaw T, Matsui T. 2004 Evidence for ocean water invasion into the Chicxulub crater at the Cretaceous/Tertiary boundary. *Met. Planet. Sci.* **39**, 1233–1247. (doi:10.1111/j.1945-5100.2004.tb00943.x)
32. Collins GS, Wünnemann K. 2005 How big was the Chesapeake Bay impact? Insight from numerical modeling. *Geology* **33**, 925–928. (doi:10.1130/G21854.1)
33. Kenkmann T, Collins GS, Wittmann A, Wünnemann K, Reimold WU, Melosh HJ. 2009 A model for the formation of the Chesapeake Bay impact crater as revealed by drilling and numerical simulations. *Geol. Soc. Am. Spec. Paper* **458**, 571–585. (doi:10.1130/2009.2458(25))
34. Lindström M, Shuvalov V, Ivanov B. 2005 Lockne crater as a result of marine-target oblique impact. *Planet. Space Sci.* **53**, 803–815. (doi:10.1016/j.pss.2005.02.005)
35. Ormö J, Miyamoto H. 2002 Computer modeling of the water resurge at a marine impact: the Lockne crater, Sweden. *Deep-Sea Res. II* **49**, 983–994. (doi:10.1016/S0967-0645(01)00143-6)
36. Glimsdal S, Pedersen GK, Langtangen HP, Shuvalov V, Dypvik H. 2007 Tsunami generation and propagation from the Mjølnir asteroid impact. *Meteorit. Planet. Sci.* **42**, 1473–1493. (doi:10.1111/j.1945-5100.2007.tb00586.x)
37. Gisler GR, Weaver RP, Mader CL, Gittings ML. 2003 Two- and three-dimensional simulations of asteroid ocean impacts. *Sci. Tsunami Hazard* **21**, 119–130.
38. Gisler GR, Weaver RP, Mader CL, Gittings ML. 2004 Two- and three-dimensional asteroid impact simulations. *Comput. Sci. Eng.* **4**, 46–55. (doi:10.1109/MCISE.2004.1289308)
39. Shuvalov V, Gersonde R. 2014 Constraints on interpretation of the Eltanin impact from numerical simulations. *Meteorit. Planet. Sci.* **49**, 1171–1185. (doi:10.1111/maps.12326)
40. Gisler RG. 2008 Tsunami simulations. *Annu. Rev. Fluid Mech.* **40**, 71–90. (doi:10.1146/annurev.fluid.40.111406.102208)
41. Crawford DA, Mader CL. 1998 Modeling asteroid impact and tsunami. *Sci. Tsunami Hazard* **16**, 21–30.
42. Ward SN. 2002 Impact tsunami-Eltanin. *Deep-Sea Res. II* **49**, 1073–1079. (doi:10.1016/S0967-0645(01)00147-3)
43. Collins GS, Wunnemann K, Artemieva N, Pierazzo B. 2013 The modification stage of crater formation. In *Impact cratering: processes and products 3* (eds GR Osinski, E Pierazzo), pp. 254–268. Oxford, UK: Wiley and Sons.
44. Weiss R, Wünnemann K, Bahlburg H. 2006 Numerical modelling of generation, propagation and run-up of tsunamis caused by oceanic impacts: model strategy and technical solutions. *Geophys. J. Int.* **167**, 77–88. (doi:10.1111/j.1365-246X.2006.02889.x)
45. Sitanggang K, Lynett P. 2005 Parallel computing of a highly nonlinear Boussinesq equation model through domain decomposition. *Int. J. Numer. Methods Fluids* **49**, 57–74. (doi:10.1002/fld.985)
46. Korycansky DG, Lynett PJ. 2005 Offshore breaking of impact tsunami: the Van Dorn effect revisited. *Geophys. Res. Lett.* **32**, L10608. (doi:10.1029/2004GL021918)
47. Korycansky DG, Lynett P. 2007 Runup from impact tsunami. *Geophys. J. Int.* **170**, 1076–1088. (doi:10.1111/j.1365-246X.2007.03531.x)
48. Weiss R, Lynett P, Wünnemann K. 2015 The Eltanin impact and its tsunami along the coast of South America: insights for potential deposits. *EPSL* **409**, 175–181. (doi:10.1016/j.epsl.2014.10.050)
49. Jacops J, Schenke HW. 2006 *Mapping of the Eltanin impact area in the South-East Pacific*. Bremerhaven, Germany: Alfred Wegener Institute, Helmholtz Center for Polar and Marine Research.
50. Kroker R. 2008 Correlation of gravimetry and bathymetry for the geologic interpretation of the Eltanin impact structure in the South Pacific. *Rept. Polar Mar. Res.* **577**, 131.